The International Journal of Advanced Manufacturing Technology (2020) 106:511–517
https://doi.org/10.1007/s00170-019-04642-w

ORIGINAL ARTICLE

Microstructure evolution of 42CrMo4 during hot forging process of hollow shafts for wind turbines

L. L. Costa[1] · A. M. G Brito[1] · A. Rosiak[1] · L. Schaeffer[1]

Received: 22 August 2019 / Accepted: 4 November 2019 / Published online: 23 November 2019

Abstract
Large parts such as shafts for wind turbines are hot forged by upset and drawing. The repetitive heating, deformation, and cooling cause different metallurgical phenomena which directly influence the material behavior during and after the forming process. Particularly, while forging these large size parts, the temperature distribution does not remain uniform. This warrants a systematic study on heating and forging workpieces at variable temperature and austenitizing times. In this work, the influence of austenitizing time and temperatures on the microstructural evolution of the 42CrMo4 steel has been investigated. Samples have been austenitized and maintained at temperatures of 900°, 1000°, 1100°, and 1200 °C for 22, 66, and 200 min each and subsequently forged and quenched. The results have shown 42CrMo4 presented a complete recrystallized microstructure only when austenitized at 1200 °C for 200 min. Microhardness profiles have shown that increasing austenitizing time combined with higher temperature decreases the microhardness values in agreement with the decrease in resulting force; thereby, the related metallurgical phenomena of recovery and recrystallization cause material softening.

Keywords 42CrMo4 · Metallurgical phenomena · Recrystallization · Grain size

1 Introduction

In the field of metal forming, the temperature is the most important factor to characterize industrial processes, among many other parameters. In case of hot forging processes in open die, the temperature distributions in workpiece and its corresponding changes over time have extremely large significance to the quality of the final forged parts [1].

In a hot forged material, the final properties are influenced by the metallurgical phenomena that occur during and after the deformation. While deformation, the phenomena of concomitant hardening and dynamic softening occur simultaneously. Dynamic softening can be of two types: dynamic recovery and dynamic recrystallization [2]. In dynamic softening, the distorted structures of the grains are quickly eliminated by the formation of new grains that are free of deformation [3]. After the deformation, restauration processes occur which result in softening of the material. There are two different phenomena that may be responsible for this softening: recovery and recrystallization [4]. These phenomena have direct influence on the final mechanical propriety in the forged parts.

The low-alloy 41XX is an important class of steels used to manufacture hot forged components such as shafts, gearing, connecting rods, crankshafts, and other which require mechanical strength, toughness to fracture and fatigue. This class of steel can present non-uniformity in mechanical properties along the forged parts, particularly in large parts such as shafts for wind turbines [5]. These steels are forged between 900 and 1250 °C [6]. The hollow shafts for wind turbines are usually manufactured using the 42CrMo4 steel. They are hot forged in open die by upset and drawing, controlled by the orientation of the mandrel in rotation, mechanical feed, and return. Schematically, Fig. 1 shows different steps to forge an industrial hollow shaft where the workpiece is elongated until the final shape of the part is obtained.

As these parts are very large, they lose heat to the air and in the contact with the dies and other tools; thereby, necessitating more than a heating during each forging step to keep them above to recrystallization temperature and maintain the hot conformability. Figure 2 presents a real hollow shaft during

✉ L. L. Costa
luana.lucca@ufrgs.br

[1] Metalforming Laboratory, Federal University of Rio Grande do Sul, Av. Bento Gonçalves, 9500, Porto Alegre 91509-900, Brazil

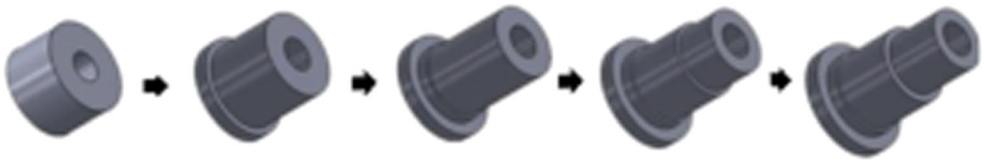

Fig. 1 Schematic representation of the steps in hot forging process to forge hollow shafts

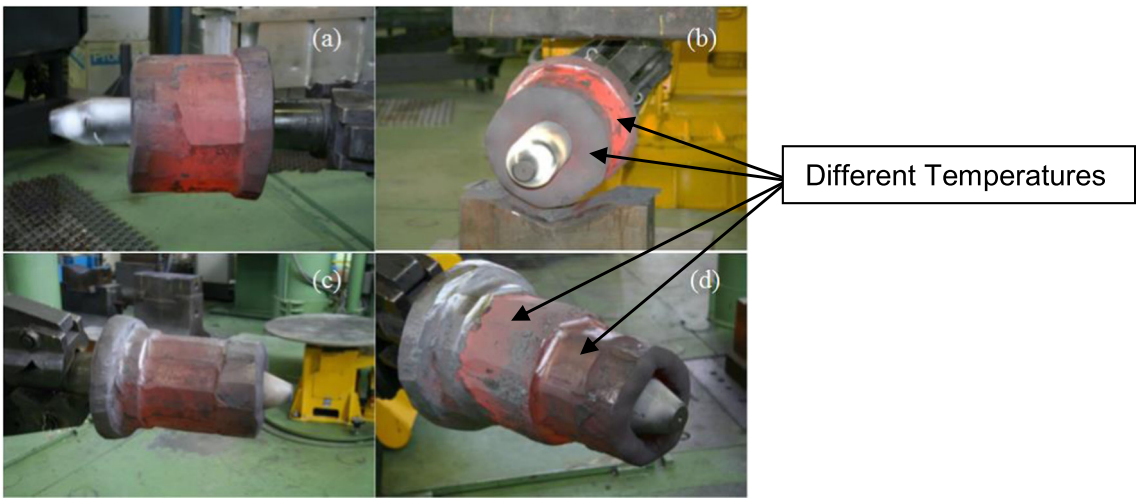

Fig. 2 Forging process in different steps (IBF-Aachen University/Germany)

forging process where regions with different temperatures can be clearly observed for the same workpiece. In addition, during hot forging process, the same workpiece also exhibits different austenitizing times. To better understand and improve the quality of the final product, it is necessary to investigate the microstructural evolution and related metallurgical phenomena as function of the heating temperature and austenitizing time.

In this research, samples of 42CrMo4 steel were hot forged in open die at different temperatures and austenitizing times to study the thermomechanical effects on microstructural evolution aiming to understand different metallurgical phenomena that occur during hot forging.

2 Experiments

The samples were manufactured by commercially available 42CrMo4 steel. For the dies was used a H13 tool steel widely applied in industry. Chemical composition of H13 tool steel and 42CrMo4 is shown in Table 1, while the experimental conditions are shown in Table 2. The samples were fabricated in cubic shape with 18 mm sides. In order to determine the temperature, 0.5-mm diameter holes were drilled up to the middle of the samples to insert a thermocouple (K-type). To investigate the metallurgical phenomena from austenitic grain, the samples were quenched. The forging process and conducted heat-treatment are displayed in Fig. 3 and Table 3.

The austenitizing temperatures were chosen according to the working temperature of large parts in hot forging process and time at the austenitizing temperature were determined by numerical simulation (FEM—finite element methods), using the software Simufact.Forming12.0®, of a 180-kg hollow shaft. These times correspond to the periods in which different

Table 1 Chemical compositions of the 42CrMo4 and H13 steels (wt%)

Material	C	Mn	P	S	Si	Cr	Mo	V
42CrMo4	0.40	0.61	0.016	0.022	0.26	0.89	0.19	–
H13	0.43	0.41	0.021	0.024	0.82	4.83	1.34	1.12

Table 2 Experimental conditions for the hot forging process

Operating variables	
Heating	Industrial electric furnace (chamber type)
Atmosphere	Air
Press	Single action hydraulic press
Maximum normal force	400 kN
Press velocity	2 mm/s
Lubrification	Graphite solution
Dies temperature	300 °C
Sample reduction height	9 mm

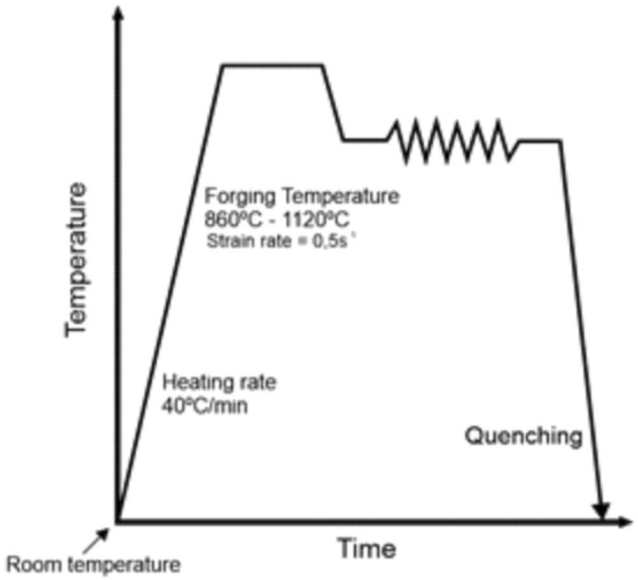

Fig. 3 Forging cycle and heat-treatment to obtain the austenitic grain

parts of the shaft remained exposed to high temperatures during the forging cycles shown schematically in Fig. 1 [7, 8].

After performing different heat treatments on the samples, the resulting microstructure was observed using an optical microscope, with application of standard metallographic techniques involving mechanical grinding and polishing. In order to reveal the austenitic grain boundaries, the samples were etched with 4 g of picric acid, 1 g of sodium tridecylbenzene sulfonate, and 1 mL of HCl dissolved in 100 mL ethanol. The solution was heated and magnetically stirred, in an ultrasound bath for approximately 7 min [9–11]. The analyses were done on the upper side of the samples. This side was chosen because based on the literature and in numerical simulations not shown in this paper, this is the region with the highest deformation. To measure microhardness, the samples were cut in the middle from the top side and a Vickers microhardness tester (at a load of 100 g for 10-s dwelling time) was used.

Table 3 Austenitizing temperature and step time

Sample	Austenitizing temperature (°C)	Time on the austenitizing temperature (min)
A	900	22
B	1000	
C	1100	
D	1200	
E	900	66
F	1000	
G	1100	
H	1200	
I	900	200
J	1000	
K	1100	
L	1200	

3 Results and discussion

The microstructure morphology of the not forged 42CrMo4 steel samples heated up to 1200 °C and quenched in saline solution is studied by the optical microscopy. The microstructure consists of equiaxial austenitic grains with clearly visible boundaries, ranging in size from 12 to 52 μm (Fig. 4). The microhardness profile of these samples resulted in hardness values between 558 and 604 HV, confirming the high hardenability of the steel. Literature reports the quenched steels with a 0.40 (wt%) of C and having 99.9% martensite present higher hardness, of ca. 613 HV suggesting the observed values of the microhardness corroborate with the reported values [12].

The micrographs of austenitic grains of the forged samples submitted to high temperature (900°, 1000°, 1100°, and 1200 °C) for an additional time longer than 22 min are compared in Fig. 5. The morphology of the grains demonstrates that the strain, strain rate, and temperature combined with the time at high temperature were not enough to accumulate the activation energy necessary for recrystallization [13].

As shown in Fig. 5, for samples A and B, there are indications of the recuperation process. This phenomenon requires low activation energy and can occur at low temperatures through small-scale structural modifications, such as punctual defects within grains [14]. It can be seen all the grains are elongated in the direction of the deformation; however, for sample B, the grains boundaries are better delimited which can be attributed to the higher temperature ca. 900 °C during forging. Higher temperatures allow the migration of the dislocation that changes the regions of higher energy (grain boundaries) which makes them visually well-defined. The recovery

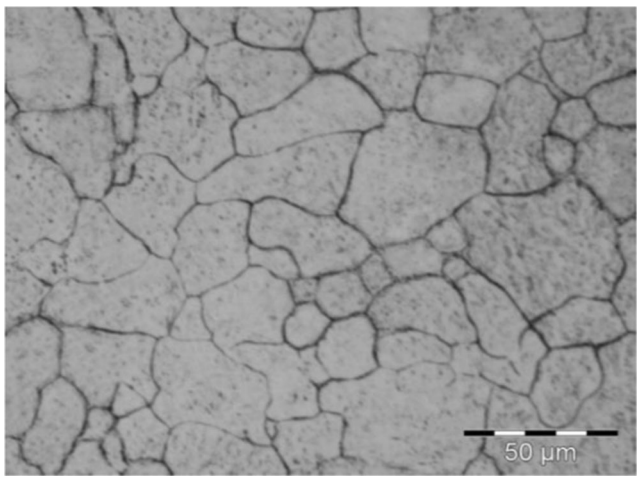

Fig. 4 Micrograph of the not forged austenitic grains

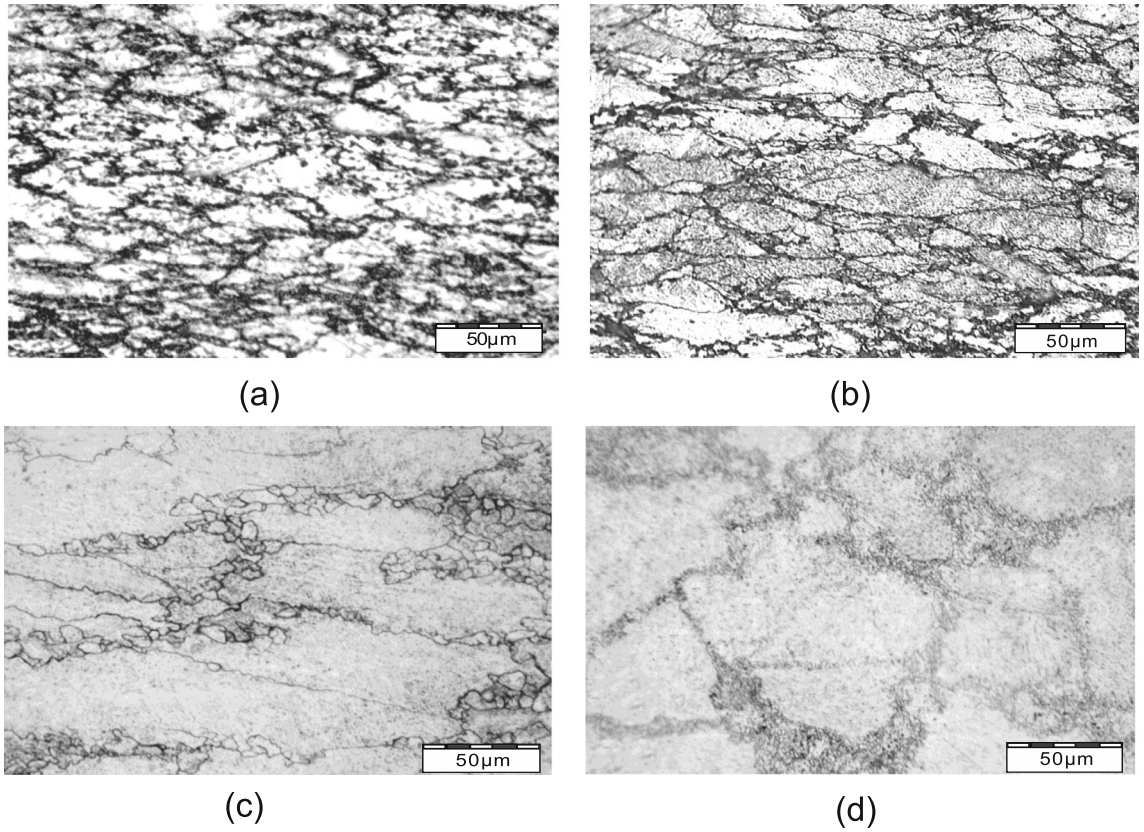

Fig. 5 Micrographics of the samples: **a** A, T = 900 °C. **b** B, T = 1000 °C. **c** C, T = 1100 °C. **d** D, T = 1200 °C

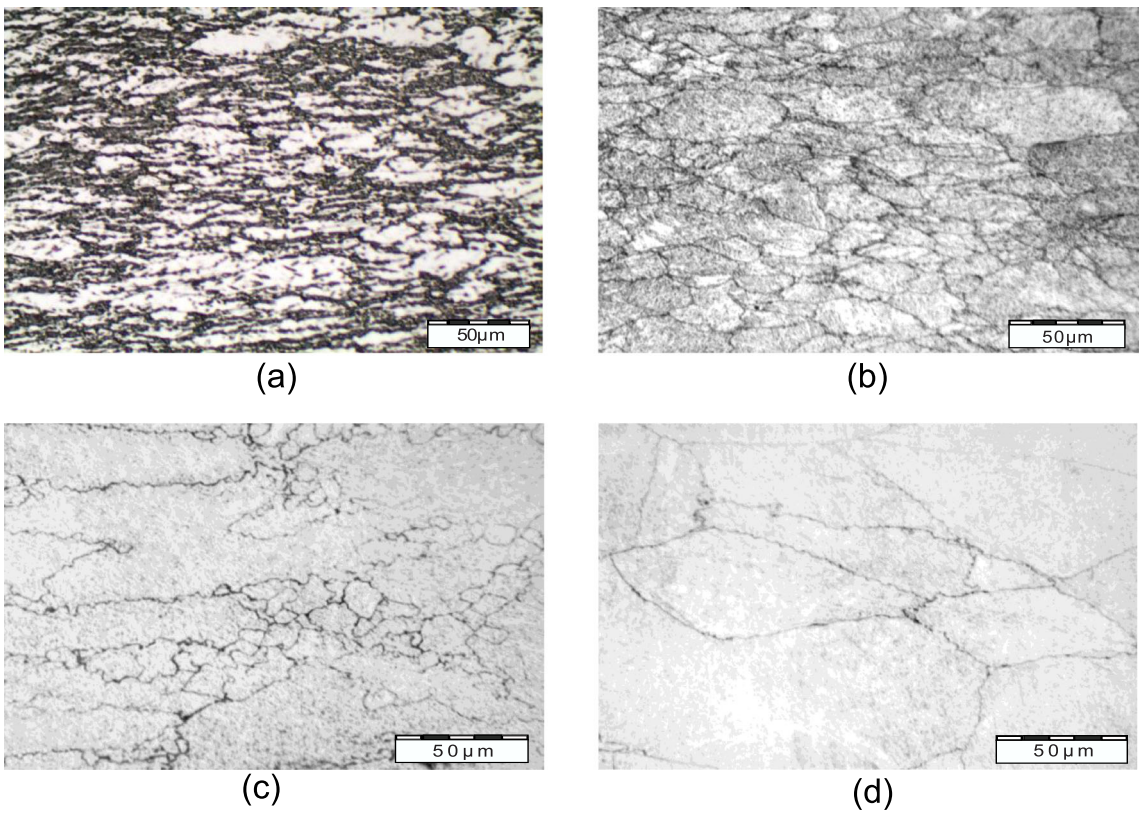

Fig. 6 Micrographics of the samples: **a** E, T = 900 °C. **b** F, T = 1000 °C. **c** G, T = 1100 °C. **d** H, T = 1200 °C

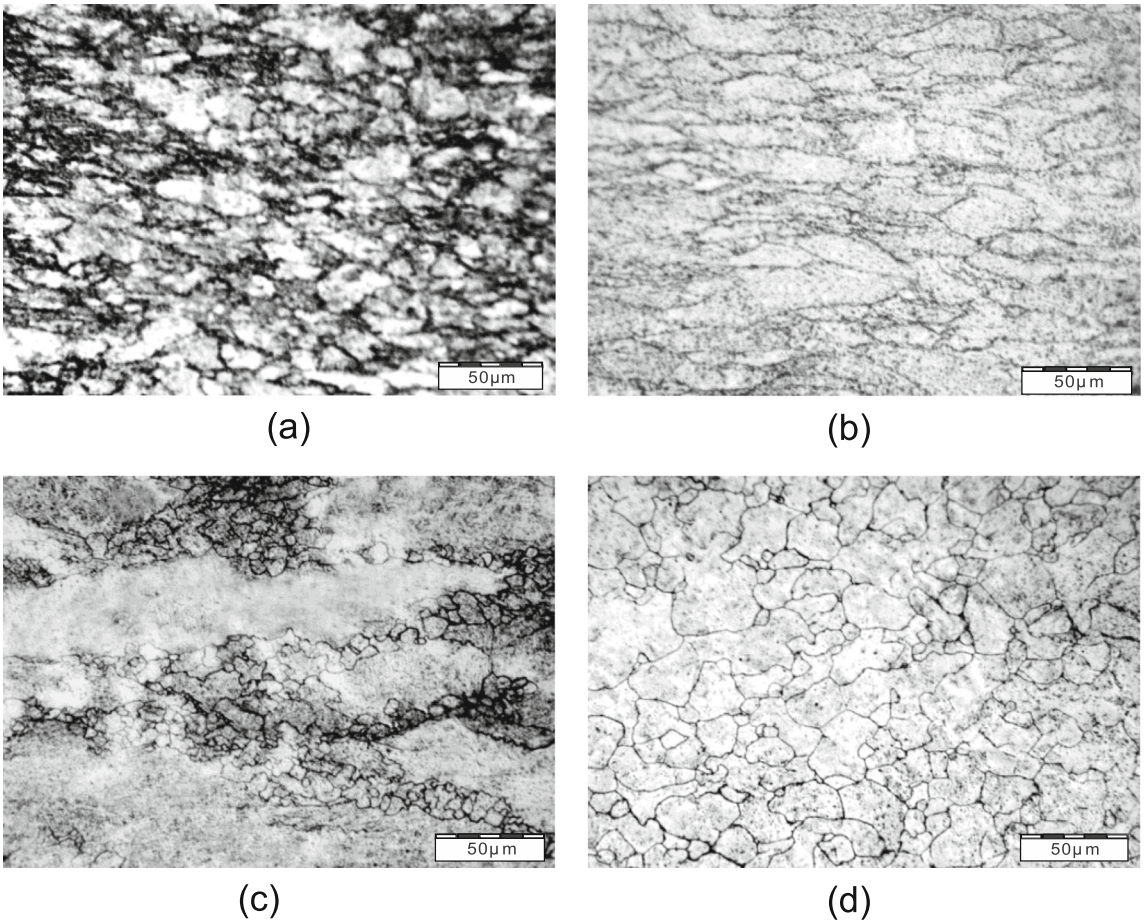

Fig. 7 Micrographics of the samples: **a** I, T = 900 °C. **b** J, T = 1000 °C. **c** K, T = 1100 °C. **d** L, T = 1200 °C

phenomenon can also be observed in the flow curves [15], where the characteristic peaks of recrystallization are not evident in these strain rate and temperatures. In sample C, recrystallized grains are observed in the boundaries of the elongated grains which is the characteristic of primary recrystallization, i.e., the migration of high angle boundaries induced by deformation. Also, the non-recrystallized grains have sizes closed to 142 μm, which are very different from the not forged sample where the values are approximately 42 μm. This phenomenon is related to the austenitizing temperature which directly influences the austenite grain size. In sample D, the nucleation of several small recrystallized grains can be

Table 4 The average values of microhardness and force necessary to forged the samples

Sample	Austenitizing temperature (°C)	Time on the austenitizing temperature (min)	Heat treatment	Microhardness (HV)	Force (kN)
A	900	22	Quenching (saline solution)	597	11.4
B	1000			474	9.5
C	1100			452	7.6
D	1200			415	6.1
E	900	66		597	11
F	1000			448	9.1
G	1100			372	7.7
H	1200			368	5.7
I	900	200		515	9.2
J	1000			460	8.2
K	1100			439	5.4
L	1200			379	4

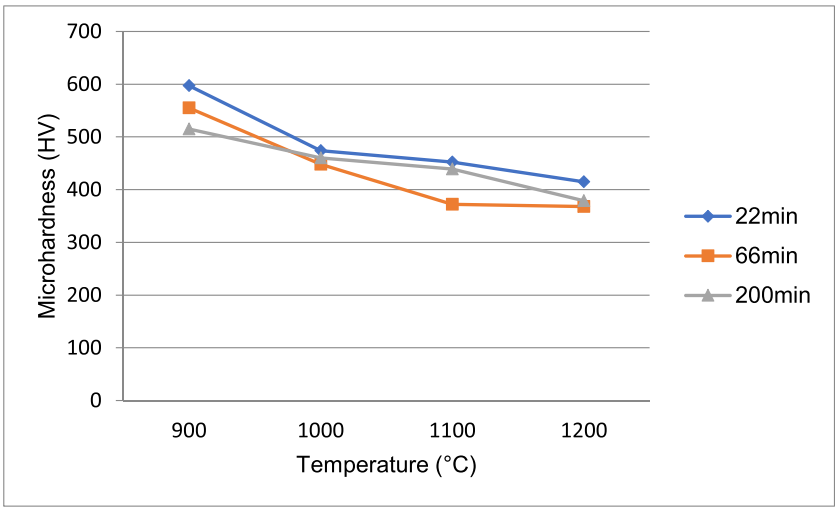

Fig. 8 Graphic representation of microhardness variation

observed which are formed due to necklacing mechanism [16, 17].

The micrographs of the samples submitted to 66 min at different austenitizing temperatures are compared in Fig. 6. These samples present a similar microstructural evolution as observed for the previous samples (Fig. 4). However, there are significant differences in the grain sizes of G samples as compared to C samples. The recrystallized grains are larger due to the longer austenitizing time and temperature which is in accordance to the 3rd and 6th Recrystallization Laws [18]. Interestingly, for H sample, the microstructure demonstrates unusual grain growth. This might be attributed to the dynamical recovery in according to the 6th Law of Recrystallization. In addition, the grains remain elongated which is not the characteristic of recrystallized grains. Therefore, the competition between recovery and recrystallization phenomena might hinder to establish which factor is dominant to form this morphology.

In relation to the micrographs of the samples submitted to 200 min in the austenitizing temperature, the results indicate that the samples followed the pattern of the previous ones (Figs. 4 and 5), except for the L samples, as shown in Fig. 7. It demonstrates the austenitizing time of the samples, from 900 to 1100 °C, did not influence the metallurgical phenomena of recrystallization; thereby, no big changes in sizes and forms of the grains were observed which is contrary to the 3rd Recrystallization Law [18].

Once temperature rises up to 1200 °C and the elapsed time is 200 min (sample L) a clear presence of equiaxial grains can be seen, which indicates the sample recrystallized. The recrystallized grains have an average size of 26 μm. Thus, the complete refining of the not forged grain by the recrystallization metallurgical phenomena occurred only in L sample forged at approximately 1120 °C.

The obtained microhardness is the result of the thermomechanical treatments to the samples. Thus, the

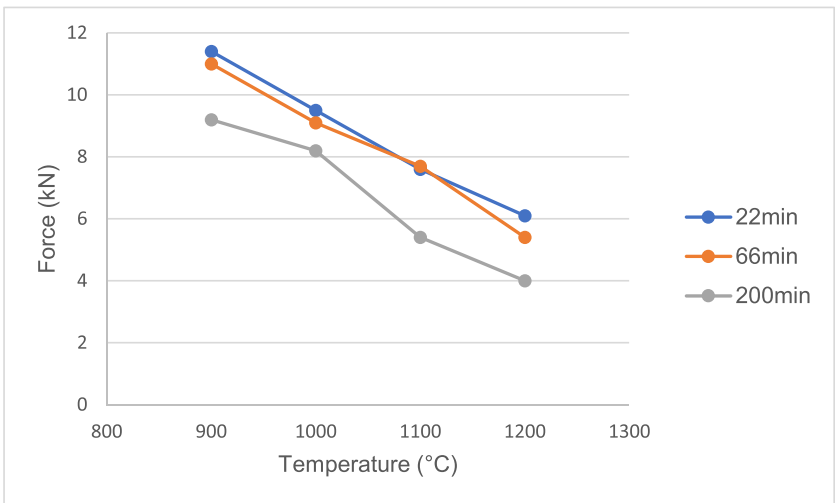

Fig. 9 Graphic representation of force variation

achievement of these results is directly related to the samples microstructure. The quenching after forging process had revealed the austenitic grain, indicating the result of these heat treatments is the martensite formation (not showed) [9]. The average values of microhardness are listed in Table 4 and compared in Fig. 8 which shows that the microhardness decreases with increase in temperature and austenitizing time that demonstrates dynamic softening in the material happens due the recovery and recrystallization phenomena.

The values of applied forces necessary to forge the samples are also listed in Table 4 and compared in Fig. 9 that show the force decreases with increase in temperature and austenitizing time. This result clearly indicates the samples are softened due to recovery and recrystallization phenomena which is in agreement to what is observed in microhardness analyses (Fig. 8). The results obtained in this study can be used to feed software database to predict the time and temperature indicated to forge large parts such as hollow shafts for wind turbines and to predict the final mechanical properties.

4 Conclusion

1. For the austenitizing temperatures of 900 and 1000 °C, the time did not significantly influence the final microstructure.
2. In D sample, nucleation of dynamically recrystallization occurs by the mechanism of necklacing.
3. The complete recrystallization phenomenon was only observed under harsh conditions of austenitizing time (200 min) and temperature (1200 °C), i.e., L sample.
4. The highest value to microhardness after forged and quenched was obtained for A sample.
5. Microhardness profile shows the decrease in hardness as a function of temperature and time of austenitizing.
6. The force necessary to forge the samples decreases as a function of the softening of the material caused by progressive metallurgical phenomena (recovery and recrystallization).
7. The microstructural evolution and the results obtained in this study can be of great utility to use in the programming database to simulate the larger industrial parts such as shafts.

Acknowledgments The authors thank the IBF – RWTH Aachen University (Germany) for the technical partnership in the project BRAGECRIM (550956/2010-7) and CNPq (National Council for Scientific and Technological Development) and Capes (Coordination for the Improvement of Higher Education Personnel) for the financial support.

References

1. Hawryluk M, Ziemba J (2017) Possibilities of application measure techniques in hot die forging processes. Measurement 110:284–285
2. Zhao P, Wang Y, Niezgoda SR (2018) Microstructural and micromechanical evolution during dynamic recrystallization. Int J Plast 100:52–68
3. Sakai T, Belyakov A, Kaibyshev R, Miura H, Jonas JJ (2014) Dynamic and post-dynamic recrystallization under hot, cold and severe plastic deformation conditions. Process in Material Science 60:130–207
4. Huang K, Logé RE (2016) A review of dynamic recrystallization phenomena in metallic materials. Mater Des 111:548–574
5. Maropoulos S, Ridley N (2004) Inclusions and fracture characteristics of HSLA steel forgings. Mater Sci Eng A 384:64–69
6. Kim SI, Lee Y, Byon SM (2003) Study on constitutive relation of AISI 4140 steel subject to large strain at elevated temperatures. J Mater Process Technol 140:84–89
7. Costa LL (2014) Efeito de diferentes ciclos termomecânicos no comportamento microestrutural do aço ABNT 4140 (In Portuguese). Porto Alegre. Dissertation, UFRGS
8. Limberger RP (2015) Estudo do forjamento de eixos vazados com contorno interno para utilização em aerogeradores (In Portuguese). Porto Alegre. Dissertation, UFRGS
9. Lui MW, May IL (1971) Etching of prior austenite grain boundaries in AlSl 4140 steel. Metallography 4(5):443–450
10. McPherson O (2008) Grain growth in AISI 4140. Massachusetts. Dissertation, Worcester Polytechnic Institute
11. Regone W (2009) Acompanhamento da evolução microestrutural no forjamento a quente com matriz fechada por simulação física e numérica (In Portuguese). Campinas. Dissertation, UNICAMP
12. Lifeng Lv FL, Ahmad S, Shang A (2017) Effect of heavy warm rolling on microstructures and mechanical properties of AISI 4140 steel. Mater Sci Eng A 704:469–479
13. Chen MS, All E (2012) The kinetics of dynamic recrystallization of 42CrMo steel. Mat Sci Eng A 556:260–266
14. Quan GZ, Li GS, Chen T, Wang YX, Zhang YW, Zhou J (2011) Dynamic recrystallization kinetics of 42CrMo steel during compression at different temperatures and strain rates. Mat Sci Eng A 528:4643–4651
15. Lin YC, Chen MS, Zong J (2008) Effect of temperature and strain rate on the compressive. J Mater Process Technol 205(1):308–315
16. Humphreys F J, Hatherly (1995) Recrystallization and related anneling fenomena. Pergamon, pp. 363-392, Oxford.
17. Padilha A F, Siciliano F (2005) Encruamento, recristalização, crescimento de grão e textura (In Portuguese). ABMM, ed. 3°: 132-149, São Paulo.
18. Burke JE, Turnbull D (1952) Recrystallization and grain growth. Progress in metal physics. Pergamon Press 3:220–292 London

Terms and Conditions

Springer Nature journal content, brought to you courtesy of Springer Nature Customer Service Center GmbH (“Springer Nature”).
Springer Nature supports a reasonable amount of sharing of research papers by authors, subscribers and authorised users (“Users”), for small-scale personal, non-commercial use provided that all copyright, trade and service marks and other proprietary notices are maintained. By accessing, sharing, receiving or otherwise using the Springer Nature journal content you agree to these terms of use (“Terms”). For these purposes, Springer Nature considers academic use (by researchers and students) to be non-commercial.
These Terms are supplementary and will apply in addition to any applicable website terms and conditions, a relevant site licence or a personal subscription. These Terms will prevail over any conflict or ambiguity with regards to the relevant terms, a site licence or a personal subscription (to the extent of the conflict or ambiguity only). For Creative Commons-licensed articles, the terms of the Creative Commons license used will apply.
We collect and use personal data to provide access to the Springer Nature journal content. We may also use these personal data internally within ResearchGate and Springer Nature and as agreed share it, in an anonymised way, for purposes of tracking, analysis and reporting. We will not otherwise disclose your personal data outside the ResearchGate or the Springer Nature group of companies unless we have your permission as detailed in the Privacy Policy.
While Users may use the Springer Nature journal content for small scale, personal non-commercial use, it is important to note that Users may not:

1. use such content for the purpose of providing other users with access on a regular or large scale basis or as a means to circumvent access control;
2. use such content where to do so would be considered a criminal or statutory offence in any jurisdiction, or gives rise to civil liability, or is otherwise unlawful;
3. falsely or misleadingly imply or suggest endorsement, approval , sponsorship, or association unless explicitly agreed to by Springer Nature in writing;
4. use bots or other automated methods to access the content or redirect messages
5. override any security feature or exclusionary protocol; or
6. share the content in order to create substitute for Springer Nature products or services or a systematic database of Springer Nature journal content.

In line with the restriction against commercial use, Springer Nature does not permit the creation of a product or service that creates revenue, royalties, rent or income from our content or its inclusion as part of a paid for service or for other commercial gain. Springer Nature journal content cannot be used for inter-library loans and librarians may not upload Springer Nature journal content on a large scale into their, or any other, institutional repository.
These terms of use are reviewed regularly and may be amended at any time. Springer Nature is not obligated to publish any information or content on this website and may remove it or features or functionality at our sole discretion, at any time with or without notice. Springer Nature may revoke this licence to you at any time and remove access to any copies of the Springer Nature journal content which have been saved.
To the fullest extent permitted by law, Springer Nature makes no warranties, representations or guarantees to Users, either express or implied with respect to the Springer nature journal content and all parties disclaim and waive any implied warranties or warranties imposed by law, including merchantability or fitness for any particular purpose.
Please note that these rights do not automatically extend to content, data or other material published by Springer Nature that may be licensed from third parties.
If you would like to use or distribute our Springer Nature journal content to a wider audience or on a regular basis or in any other manner not expressly permitted by these Terms, please contact Springer Nature at

onlineservice@springernature.com